UDC 621.313 https://doi.org/10.20998/2074-272X.2026.2.09

A. Nayli, S. Guizani, F. Ben Ammar

Normal and degraded operation of the open-end winding induction machine fed by 2-level inverters in cascading

Introduction. *The machine-converter system is a prevalent and essential configuration, widely used not only in variable-speed industrial drive applications, but also in high-tech transportation and power fields.* ***Problem.*** *Conventional drive systems, particularly those supplied by standard 2-level inverters, face major challenges regarding the enhancement of their dynamic performance and drive availability. To overcome these limitations, a solution involves utilizing the open-end stator winding induction machine associated with cascaded 2-level inverter topologies. The* ***goal*** *of this work is to improve the availability of the drive system by increasing its degrees of freedom through the association of an open-end winding induction machine by two cascaded 2-level inverters.* ***Methodology.*** *The mathematical modeling of this machine is presented and validated using MATLAB/Simulink. To evaluate the machine's performance, it is first powered by two cascaded 2-level inverters and subsequently by three cascaded 2-level inverters. Following this initial evaluation, the machine is then fed by two cascaded 2-level inverters operating in degraded mode. This analysis features different failure configurations, and the specific operational conditions that must be respected.* ***Results.*** *This topology enhances dynamic performances and enables effective power segmentation as well as a degraded mode operation. These benefits are confirmed by the simulation results. The* ***scientific novelty*** *is based on demonstrating the effectiveness of degraded mode control, which gives the machine-cascaded inverters topology a superior advantage in terms of reliability and performances.* ***Practical value.*** *This topology provides a highly reliable and fault-tolerant drive solution, ensuring better performance during normal operation and better availability after an inverter failure.* References 15, tables 1, figures 24.

Key words: **open-end winding induction machine, cascaded 2-level inverters, degraded mode, power segmentation.**

Вступ. *Система «машина-перетворювач» є поширеною та важливою конфігурацією, що широко використовується не тільки в системах приводу з регульованою швидкістю в промисловості, а й у високотехнологічних транспортних та енергетичних галузях.* ***Проблема***. *Традиційні системи приводу, особливо ті, які живляться від стандартних дворівневих інверторів, стикаються із серйозними проблемами щодо підвищення їх динамічних характеристик та доступності приводу. Для подолання цих обмежень пропонується рішення, що включає використання асинхронної машини з відкритою статорною обмоткою в поєднанні з каскадними дворівневими інверторними топологіями.* ***Мета*** *роботи – підвищення доступності системи приводу за рахунок збільшення її ступенів свободи шляхом з'єднання асинхронної машини з відкритою обмоткою з двома каскадними дворівневими інверторами.* ***Методика***. *Математична модель цієї машини розроблена та перевірена за допомогою MATLAB/Simulink. Для оцінки продуктивності машини спочатку живлять її від двох каскадних дворівневих інверторів, а потім від трьох каскадних дворівневих інверторів. Після початкової оцінки машина живиться від двох каскадно з'єднаних дворівневих інверторів, що працюють у режимі зниженої потужності. Цей аналіз включає різні зміни відмов і конкретні умови експлуатації, яких необхідно дотримуватися.* ***Результати***. *Дана топологія підвищує динамічні характеристики та забезпечує ефективне сегментування потужності, а також роботу в режимі зниженої потужності. Ці переваги підтверджуються результатами моделювання.* ***Наукова новизна*** *ґрунтується на демонстрації ефективності управління в режимі зниженої потужності, що дає топології «машина-каскадні інвертори» значну перевагу з погляду надійності та продуктивності.* ***Практична цінність***. *Дана топологія забезпечує високонадійне та відмовостійке рішення для приводу, гарантуючи кращу продуктивність у нормальному режимі роботи та кращу доступність після відмови інвертора.* Бібл. 15, табл. 1, рис. 24.

Ключові слова: **асинхронна машина з відкритою обмоткою, каскадні дворівневі інвертори, режим зі зниженою потужністю, сегментація потужності.**

Introduction. In order to satisfy the demands for reliability, availability and dynamic performance of the drive system across various industrial domains [1–3], power segmentation at the level of the machines is often used [4–6]. This approach specifically allows for the optimization of electrical system performance by simultaneously increasing reliability, modularity, scalability and reconfigurability, while also ensuring better cost control; ultimately, adopting this strategy yields cleaner power waveforms and minimizes stress on power semiconductor devices, thereby substantially enhancing the overall efficiency and durability of the drive system. Consequently, several lines of research have focused on inverter structures such as 2-level cascaded inverters and various other multilevel topologies [7, 8] as well as on machine structures including multiphase machines [9, 10], double-star machines, where each star is supplied by its own 3-phase voltage source inverter [11–13], this architecture substantially enhances the drive system's reliability, providing multiple degrees of redundancy [4]. Another machine structure is the open-end winding induction machine (OEWIM), where each end is supplied by its own 3-phase voltage source inverter [5, 14, 15].

The **goal** of this work is to improve the availability of the drive system by increasing its degrees of freedom through the association of an open-end winding induction machine by two cascaded 2-level inverters.

The structure of the work is next. In the first part, the mathematical modeling of the proposed OEWIM is presented and implemented in the MATLAB/Simulink. In the second part, the OEWIM is fed by cascaded 2-level inverter structures based on a pulse width modulation (PWM) strategy. The various results obtained concerning the speed, torque, stator current, the voltage between phases of the cascaded inverters and the machine, the total harmonic distortion (THD) of the voltage and the torque ripple are shown. The final part of this work presents the machine's degraded mode performance across 4 specific inverter failure configurations, utilizing two cascaded 2-level inverters. Successfully conducting this study requires strict adherence to predefined operational constraints unique to each configuration.

Modeling of the OEWIM. As shown in Fig. 1, the design of the OEWIM allows for a dual-inverter supply configuration.

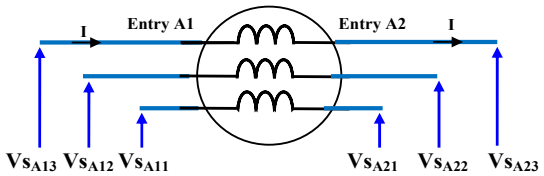

Fig. 1. The design of o the OEWIM

© A. Nayli, S. Guizani, F. Ben Ammar

The following state equations describe the mathematical flux model in the (d, q) reference frame:

$$\begin{cases} \dfrac{\mathrm{d}X(t)}{\mathrm{d}t} = [\boldsymbol{A}]\cdot[\boldsymbol{X}(t)] + [\boldsymbol{B}]\cdot\boldsymbol{U}(t); \\ \boldsymbol{Y}(t) = [\boldsymbol{C}]\cdot\boldsymbol{X}(t), \end{cases} \quad (1)$$

where the state vector:

$$\boldsymbol{X}(t) = [\boldsymbol{\Phi}] = \begin{bmatrix} \Phi_{\mathrm{sd}} & \Phi_{\mathrm{sq}} & \Phi_{\mathrm{rd}} & \Phi_{\mathrm{rq}} \end{bmatrix}^T;$$

the control vector:

$$\boldsymbol{U}(t) = U_1(t) - U_2(t) = \begin{bmatrix} V_{\mathrm{sd1}} - V_{\mathrm{sd2}} & V_{\mathrm{sq1}} - V_{\mathrm{sq2}} \end{bmatrix}^T;$$

the output vector:

$$\boldsymbol{Y}(t) = [\boldsymbol{I}] = \begin{bmatrix} I_{\mathrm{sd}} & I_{\mathrm{sq}} & I_{\mathrm{rd}} & I_{\mathrm{rq}} \end{bmatrix}^T.$$

The equation of current vector is:

$$[\boldsymbol{I}] = [\boldsymbol{L}]^{-1}[\boldsymbol{\Phi}]. \quad (2)$$

The matrices [$\boldsymbol{A}$], [$\boldsymbol{B}$] and [$\boldsymbol{C}$] are:

$$[\boldsymbol{A}] = \begin{bmatrix} -\dfrac{1}{\sigma\tau_s} & \omega_{dq} & \dfrac{L_m}{\sigma\tau_s L_r} & 0 \\ -\omega_{dq} & -\dfrac{1}{\sigma\tau_s} & 0 & \dfrac{L_m}{\sigma\tau_s L_r} \\ \dfrac{L_m}{\sigma\tau_r L_s} & 0 & -\dfrac{1}{\sigma\tau_r} & \omega_{dq}-\omega \\ 0 & \dfrac{L_m}{\sigma\tau_r L_s} & -(\omega_{dq}-\omega) & -\dfrac{1}{\sigma\tau_r} \end{bmatrix}; \quad (3)$$

$$[\boldsymbol{B}] = \begin{bmatrix} 1 & 0 & 0 & 0 \\ 0 & 1 & 0 & 0 \\ 0 & 0 & 1 & 0 \\ 0 & 0 & 0 & 1 \end{bmatrix}; \quad (4)$$

$$[\boldsymbol{C}] = [\boldsymbol{L}]^{-1} = \begin{bmatrix} \dfrac{1}{\sigma L_s} & 0 & \dfrac{-L_m}{\sigma L_s L_r} & 0 \\ 0 & \dfrac{1}{\sigma L_s} & 0 & \dfrac{-L_m}{\sigma L_s L_r} \\ \dfrac{-L_m}{\sigma L_r L_s} & 0 & \dfrac{1}{\sigma L_r} & 0 \\ 0 & \dfrac{-L_m}{\sigma L_r L_s} & 0 & \dfrac{1}{\sigma L_r} \end{bmatrix}, \quad (5)$$

where $\tau_s = L_s/R_s$, $\tau_r = L_r/R_r$ are the constants of time for stator and rotor; R_s, R_r are the resistances of stator and rotor; L_s, L_r are the inductances of stator and rotor; $\sigma = 1 - (L_m^2/L_s{\cdot}L_r)$ is the coefficient of dispersion of Blondel; L_m is the mutual inductance between stator and rotor.

The mechanical equation governing the drive and the electromagnetic torque T_{em} is:

$$T_{em} - T_r = j\frac{\mathrm{d}\omega}{\mathrm{d}t} + f\omega; \quad (6)$$

$$T_{em} - T_r = \frac{3}{2}p\left(\psi_{s\alpha}I_{s\beta} - \psi_{s\beta}I_{s\alpha}\right), \quad (7)$$

where T_r is the load torque; f is the frequency; ω is the angular frequency; p is the number of pairs of poles; $\psi_{s\alpha}$, $\psi_{s\beta}$, $I_{s\alpha}$, $I_{s\beta}$ are the flux linkages and the stator currents in the (α, β) reference frame.

Supply of the OEWIM by two cascaded 2-level inverters. The OEWIM is fed by two cascaded 2-level inverters based on PWM, with each inverter drawing power from a quarter of the DC-link voltage (E/4) (Fig. 2).

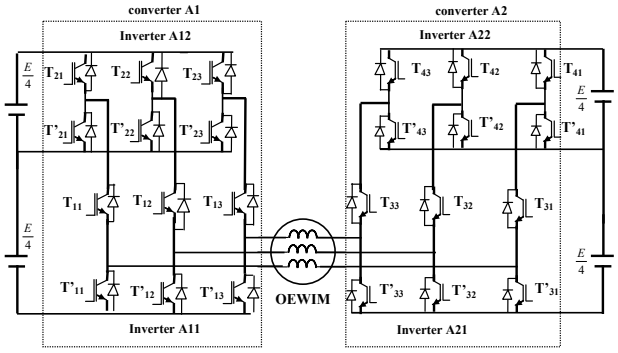

Fig. 2. Supply the OEWIM by two cascaded 2-level inverters

The evolution of the stator currents, speed and torque is shown in Fig. 3, illustrating the transient and steady-state modes during normal operation. The load torque is the type $k\omega^2$.

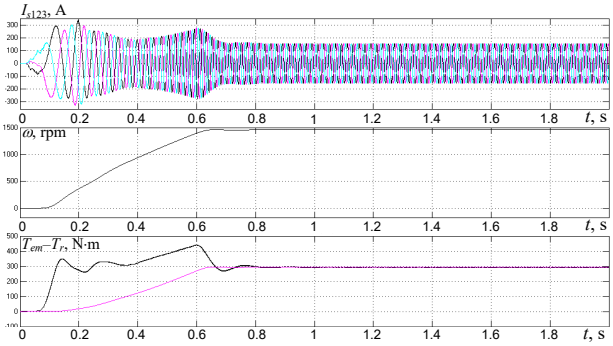

Fig. 3. Evolution of the stator currents, speed and torque

Figure 4 provides an enlarged view of the torque under steady-state conditions.

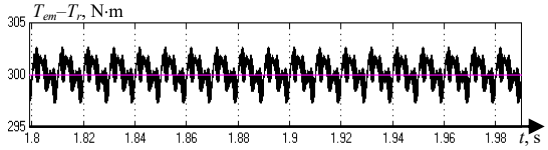

Fig. 4. Enlarged view of the torque

The torque ripple is calculated as:

$$\Delta T_{\mathrm{em}} = \frac{302.65 - 300}{300}\cdot 100\% = 0.88\%.$$

Figure 5 shows the compound voltages in the steady-state regime during normal operation. Specifically, the voltages at stator input A1 (U_1=Vs_{11}–Vs_{12}) of converter A1 and at input A2 (U_2=Vs_{21}–Vs_{22}) of converter A2 are shown. The machine phase-to-phase voltage U_{A}, which is given by the difference U_{A}=U_1–U_2, features 5 voltage levels.

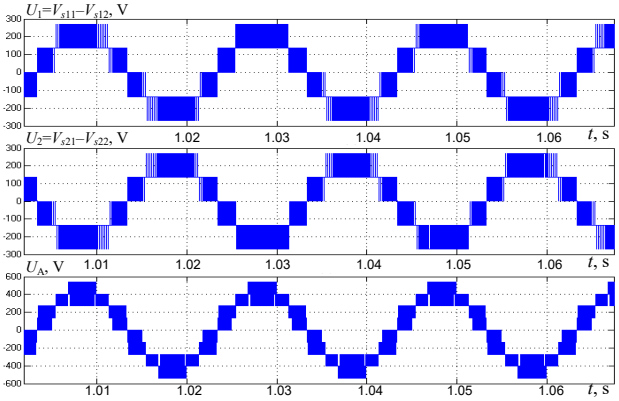

Fig. 5. Compound voltages at the terminals of the two cascaded 2-level inverters and the machine

THD of the voltage across the machine terminals is 24.99 % (Fig. 6).

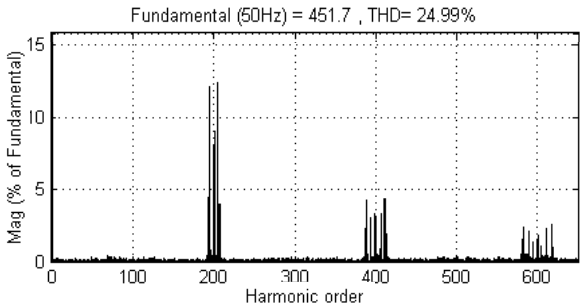

Fig. 6. THD of the machine voltage

The use of cascaded 2-level inverters to power the machine significantly increases the phase-to-phase voltage level from 3 to 5 levels when compared to conventional converters with the same machine. This configuration also substantially improves the voltage THD and doubles the bandwidth relative to a classic induction machine [4].

Supply of the OEWIM by three cascaded 2-level inverters. As illustrated in Fig. 7, the OEWIM is powered by three cascaded 2-level inverters. Crucially, each inverter is supplied by a dedicated DC source equivalent to 1/6 of the total DC-link voltage (E/6).

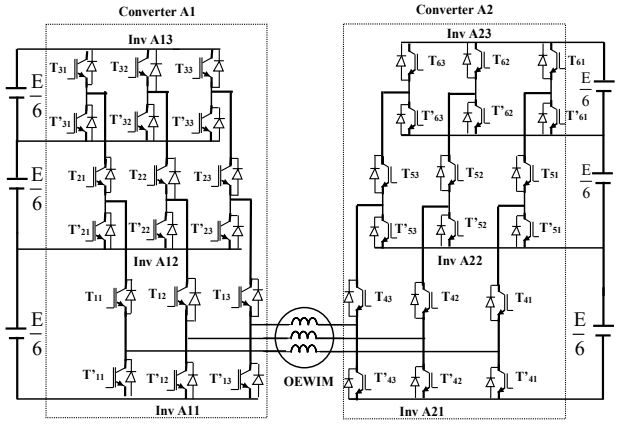

Fig. 7. Supply the OEWIM by three cascaded 2-level inverters

Figure 8 provides an enlarged view of the torque under steady-state conditions.

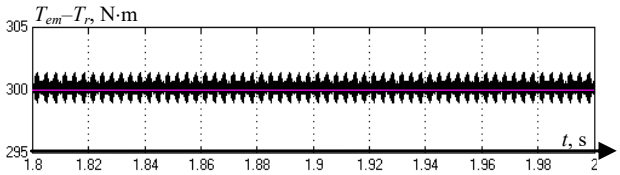

Fig. 8. Enlarged view of the torque

The steady-state torque ripple was calculated as follows: $\Delta T_{\text{em}} = \dfrac{301.35 - 300}{300} \cdot 100\% = 0.45\%$

Figure 9 shows a detailed visualization of the compound voltages in the steady-state regime during normal operation. It clearly differentiates the 4-level voltage waveform observed at the converter terminals from the 7-level voltage waveform observed at the machine terminals.

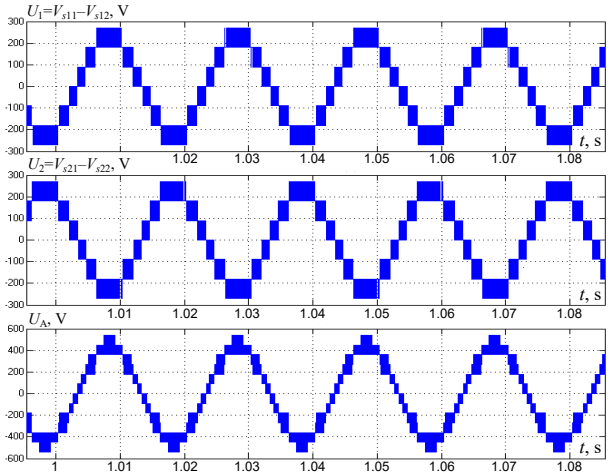

Fig. 9. Compound voltages at the terminals of the three cascaded 2-level inverters and the machine

THD of the voltage across the machine terminals is 15.07 % (Fig. 10).

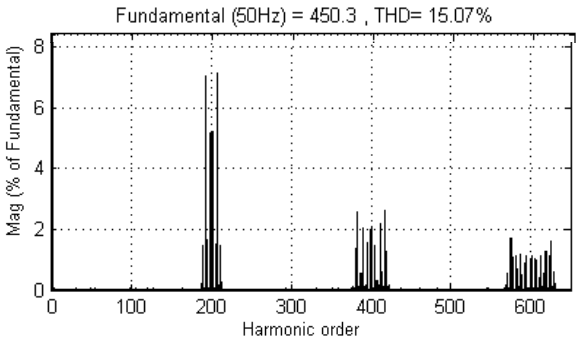

Fig. 10. THD of the machine voltage

The performance characteristics for different cascaded converters are detailed in Table 1. Specifically, the table reports the voltage levels at converter A1, A2 and OEWIM terminals, the voltage harmonic distortion rate and the steady-state torque ripple.

Table 1

Different results of THD and torque ripple

Voltage levels			THD of the voltage, %	ΔT_{em}, %
Inverter A1	Inverter A2	Machine N		
3	3	5	24.99	0.88
4	4	7	15.07	0.45

The integration of cascaded 2-level inverters with the OEWIM configuration delivers substantial performance enhancements across the drive system. Chief among these is the ability to increase the phase-to-phase voltage resolution from 5 to 7 levels, depending on the cascaded inverter topology employed. This voltage resolution directly translates into quantifiable improvements in signal quality. The voltage THD is drastically reduced from 24.99 % to 15.07 %, and the torque quality is improved, decreasing from 0.88 % to 0.45 %.

Degraded mode operation for the OEWIM fed by two cascaded 2-level inverters. Our focus is the degraded-mode operation of the OEWIM, which is powered by two 3-level converter systems. As each system comprises two cascaded 2-level inverters, we investigate 4 potential fault configurations by considering

only failures within the converter feeding input A1, given the operational symmetry with input A2. These 4 configurations stem from the fault location (upper or lower stage) in each of the 2 cascaded inverters. The specific operational constraints for each configuration must be adhered to throughout the study.

Sizing inverters. Accurate sizing of cascaded 2-level inverters is a prerequisite for proposing a mitigation strategy during degraded-mode operation. This section demonstrates the relevant sizing criteria based on the configuration of two cascaded 2-level inverters (Fig. 11).

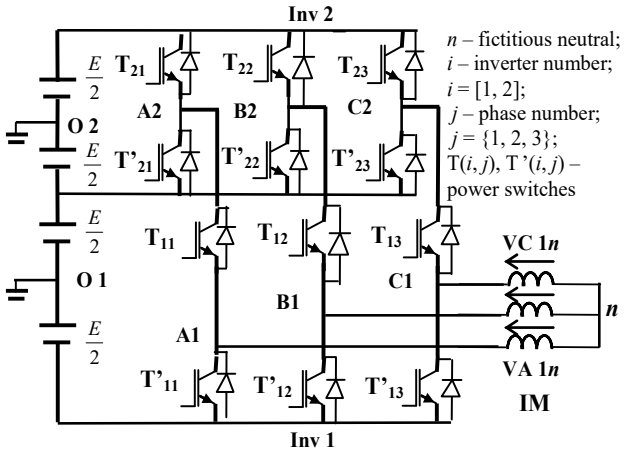

Fig. 11. Induction machine fed by two cascaded 2-level inverters

As shown in Fig. 11, the DC bus voltage for each inverter is denoted by E. This allows us to define the relation as follows. For inverter 2:

$$V_{\mathrm{T'}_{21}} = \frac{E}{2} + V_{\mathrm{A2O2}} = \frac{E}{2} + \frac{E}{2} = E\,. \qquad (8)$$

For inverter 1:

$$V_{\mathrm{T'}_{11}} = \frac{3E}{2} + V_{\mathrm{A2O2}} = \frac{3E}{2} + \frac{E}{2} = 2E\,. \qquad (9)$$

In this configuration, the OEWIM is sized for a power P. Since the machine is powered at each input by two cascaded 2-level inverters, the required sizing is:

- inverters Inv A11 and Inv A21 are rated for a power $P/2$;
- inverters Inv A12 and Inv A22 are rated for $P/4$.

Different configurations. We consider the failures of the converter A1 (the behavior is identical for failures of the converter A2). Only one fault is considered at a time. Four configurations 1–4 are possible.

Configuration 1. In the 1st configuration (Fig. 12) we consider an open circuit of one of the switches: T_{11} or T_{12} or T_{13} of the inverter A11 (following a short circuit). The control must act so that the 3 switches T_{11}, T_{12} and T_{13} are in state 0 and the switches T'_{11}, T'_{12} and T'_{13} are in state 1. We will thus have a star coupling of the input A1 of the machine.

This is the operation of the classic induction machine powered by converter A2. The machine must operate at reduced speed and therefore there are no conditions on the sizing of the inverters:

- 70 % of the nominal speed for $T_r = k\omega^2$;
- 50 % of the nominal speed for $T_r = k\omega$.

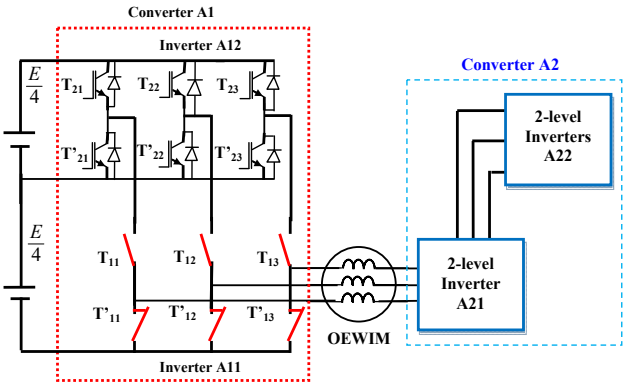

Fig. 12. Supply the OEWIM by cascaded 2-level inverters for the configuration 1

The provided figures illustrate the simulated operation of an OEWIM powered by two cascaded 3-phase inverters. The simulation is designed to show the machine's behavior before and after a fault that occurs at t = 1.2 s in inverter A11. The system has a load torque defined by the equation $T_r = k\omega^2$. This particular characteristic necessitates a control strategy that intentionally commands the machine's speed to drop to 70 % of its nominal value following the fault. As shown in Fig. 13, this speed reduction is imposed at the moment of the fault, which effectively reducing the required torque to manage the load and allowing the machine to operate safely despite the inverter failure.

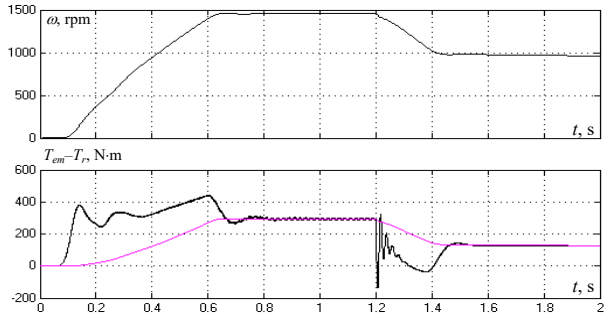

Fig. 13. Evolution of speed and torque for the configuration 1

Figure 14 shows the evolution of the stator currents before and after the failure in the inverter A11, which occurs alongside a reduction in speed.

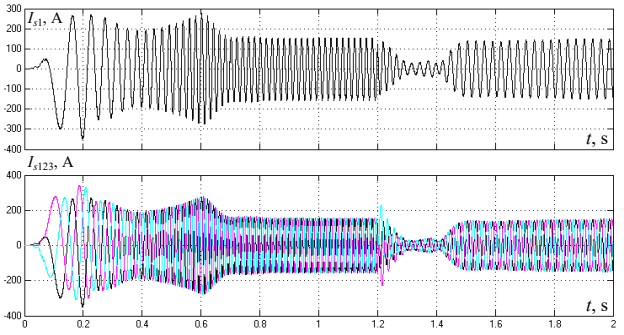

Fig. 14. Evolution of stator current for configuration 1

Figure 15 shows the evolution of the machine and inverter voltages, covering the regimes before and after the failure that occurred within inverter A11. A zoomed visualization is included to accurately capture the immediate dynamic response of the system to the fault.

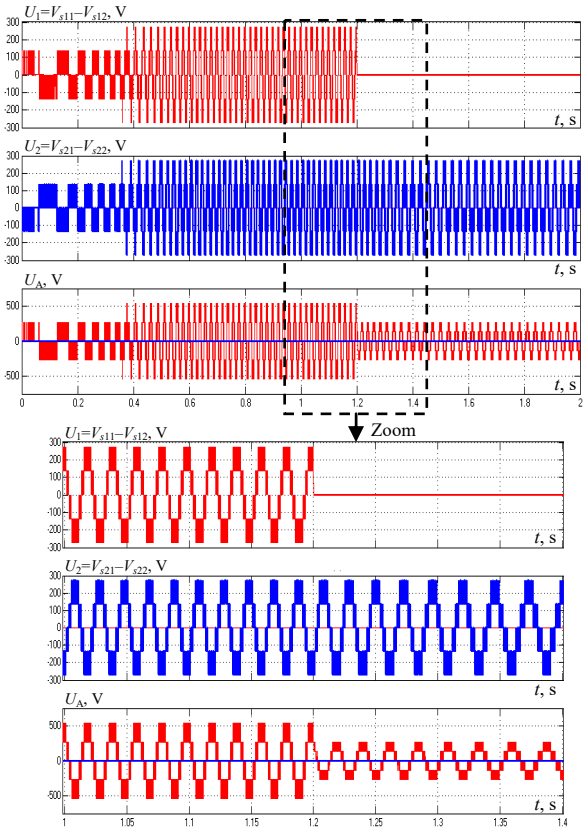

Fig. 15. Evolution of the machine and inverter voltages for configuration 1

Configuration 2. In the 2nd configuration (Fig. 16) we consider an open circuit in one of the switches of inverter A11 (T'_{11}, T'_{12}, or T'_{13}). Following a short circuit event, the control system must act to force the affected switches (T'_{11}, T'_{12}, and T'_{13}) to state 0 and their complementary switches (T_{11}, T_{12}, and T_{13}) to state 1. For this configuration, the machine is powered through its input 2 and exclusively by the A12 inverter. Following the failure of inverter A11, the OEWIM shifts into a fault-tolerant mode where it is supplied only by the remaining inverters (A12, A21 and A22). This operational change means the machine is now fed by the sum of 3 continuous DC buses, resulting in a total DC-link voltage $3E/4$. This constrained voltage supply directly limits the maximum operational speed the machine can achieve while delivering the required load torque. Consequently, the machine must operate at a reduced maximum speed: this speed is 86 % of the nominal value for quadratic load torque $T_r = k\omega^2$, or is further restricted to 75 % of the nominal speed for linear load torque $T_r = k\omega$.

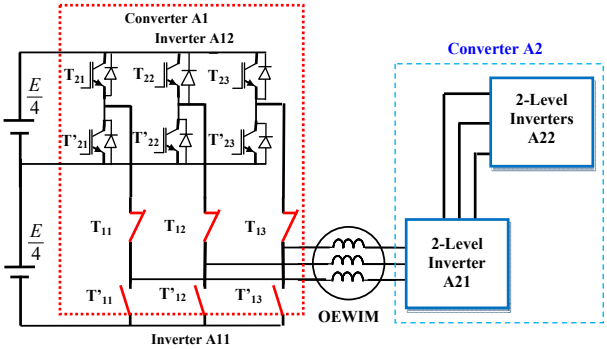

Fig. 16. Supply the OEWIM by cascaded 2-level inverters for configuration 2

Figure 17 presents the evolution of speed and torque with a speed reduction to 86 % of the nominal speed to maintain the operating current for $T_r = k\omega^2$.

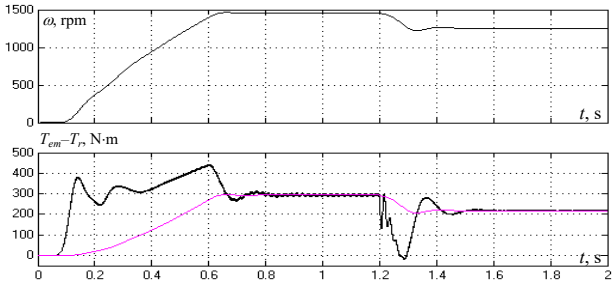

Fig. 17. Evolution of speed and torque for configuration 2

Figure 18 shows the evolution of the stator currents during an event accompanied by a reduction in speed.

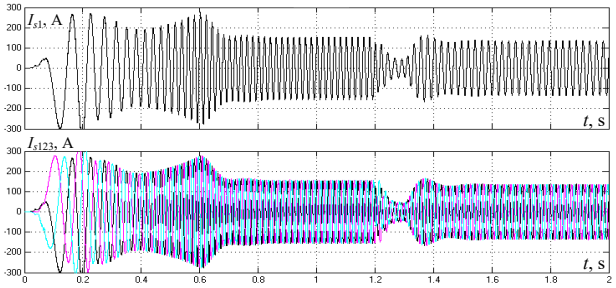

Fig. 18. Evolution of stator current for configuration 2

Figure 19 shows the evolution of the machine and inverter voltages in both normal and degraded operating modes. A zoomed visualization provides a detailed view to better capture the immediate impact of the fault that occurred at t = 1.2 s in inverter A11.

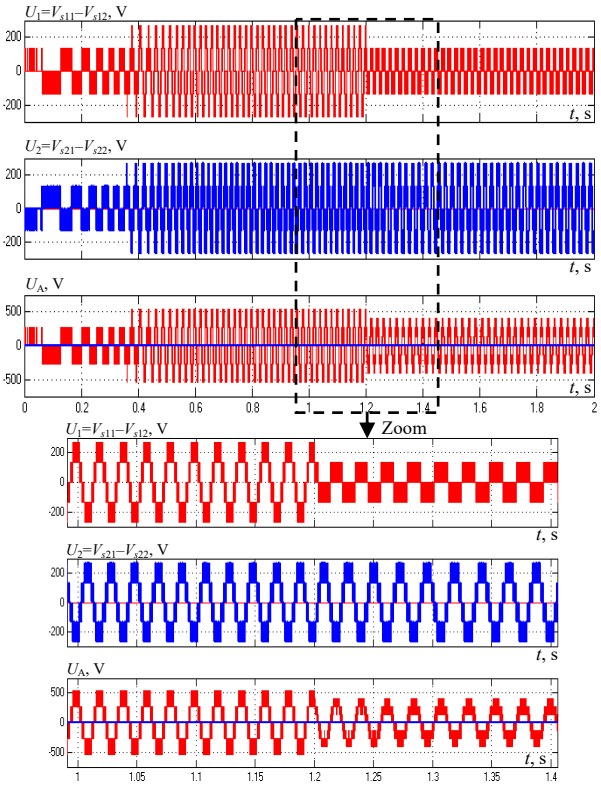

Fig. 19. Evolution of the machine and inverter voltages for configuration 2

Configuration 3. For the 3rd configuration (Fig. 20) we consider an open-circuit fault on one of the switches (T_{21}, T_{22}, or T_{23}) of inverter A12. The control system must then act by ensuring that the 3 switches (T_{11}, T_{12}, and T_{13}) are set to state 0 and switches (T'_{21}, T'_{22}, and T'_{23}) are set to state 1. The input A1 of the machine is powered by only inverter A11. We will have the same power supply conditions as in the 2nd configuration, where the power supply to input A1 is provided solely by inverter A12. Moreover, in both cases, the DC bus voltage at input A1 is $E/4$, the results are then identical to those obtained in the 2nd configuration.

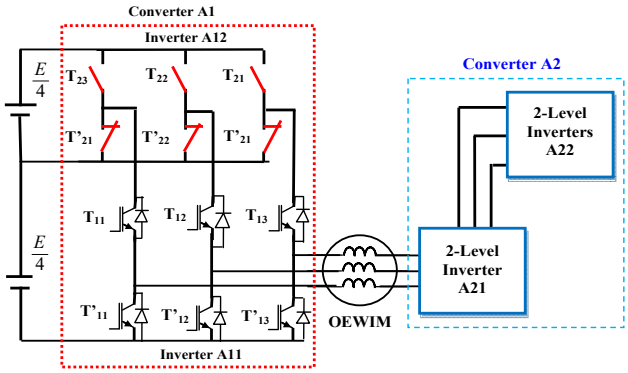

Fig. 20. Supply the OEWIM by cascaded 2-level inverters for the configuration 3

Configuration 4. The 4th configuration involves an open-circuit fault on switch (T'_{21}, T'_{22}, or T'_{23}) of inverter A12. Consequently, the control sets switches (T'_{21}, T'_{22} and T'_{23}) to state 0 and switches (T_{21}, T_{22}, and T_{23}) to state 1 (Fig. 21). Since the DC bus voltage at input A1 is now $E/2$, the machine operates at nominal speed. No operating conditions need to be imposed on inverter A11, as it is sized for half of the nominal power.

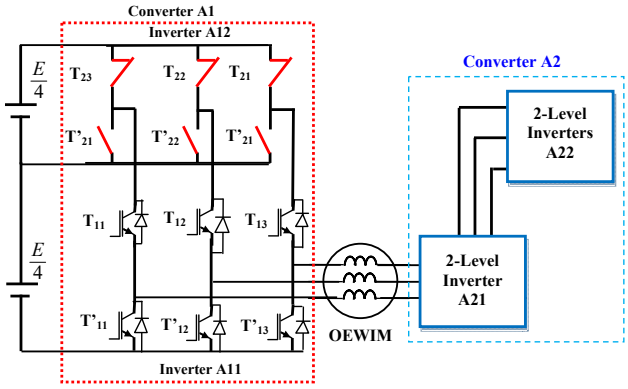

Fig. 21. Supply the OEWIM by cascaded 2-level inverters for configuration 4

The evolution of the speed and torque after the inverter A11 failure is shown in Fig. 22. The results display the state before and after the fault at t = 1.2 s, maintaining 100 % of the nominal speed with a load torque of $T_r = k\omega^2$.

Figure 23 shows the evolution of the stator currents before and after the failure of inverter A12, demonstrating that the stator current magnitude remains unchanged (or similar) despite the fault.

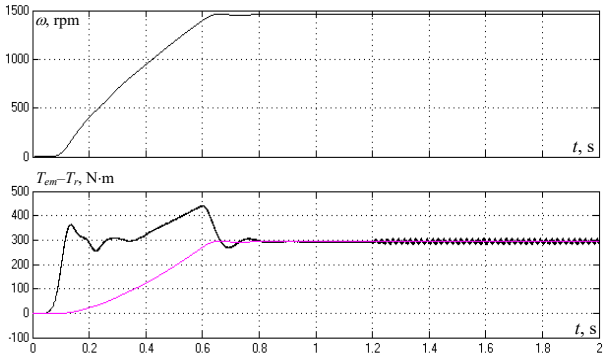

Fig. 22. Evolution of the speed and torque for configuration 4

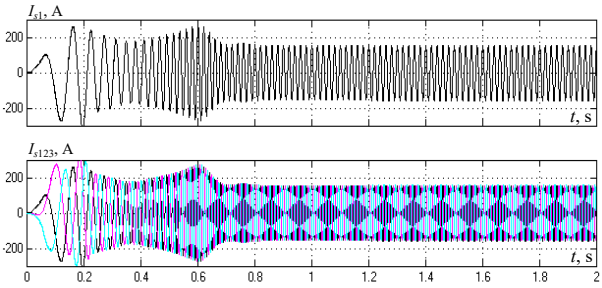

Fig. 23. Evolution of stator current for configuration 4

The evolution of the machine and inverter voltages before and after a failure in inverter A11 at t = 1.2 s is shown in Fig. 24. This event occurred while the DC bus voltage at input A1 is $E/2$. A zoomed view provides a detailed visualization to better capture the immediate impact of the fault.

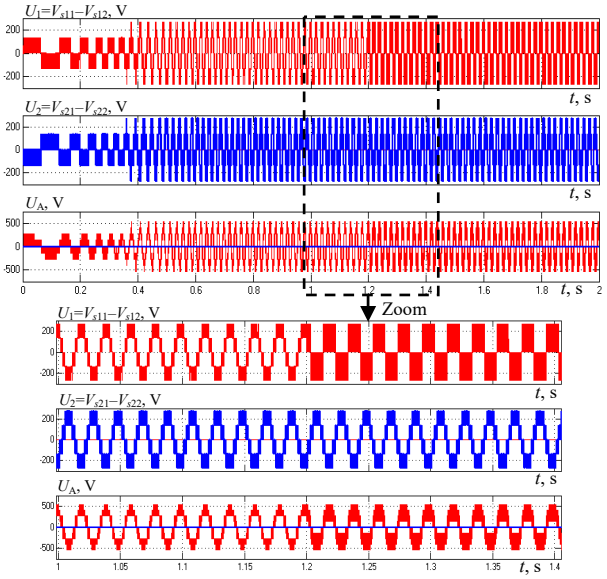

Fig. 24. Evolution of the machine and inverter voltages for configuration 4

The characteristics of the machine, which has a nominal power P = 45 kW, are defined by: nominal speed of 1450 rpm, stator resistance R_s = 150 mΩ, rotor resistance R_r = 46 mΩ, stator inductance L_s = 17.9 mH, rotor inductance L_r = 18.6 mH, mutual inductance L_m = 17.2 mH.

Conclusions. The association of the OEWIM with cascaded 2-level inverter structures offers benefits in both operating modes. In normal mode, it improves dynamic performances. In degraded mode, it enhances the system's reliability, availability, and safety because the failure of a single inverter does not stop the motor.

The OEWIM mathematical model was derived and simulated using the MATLAB/Simulink. The results obtained allowed us to draw the following conclusions: for the normal operation, supplying the machine with cascaded 2-level inverter structures offers several advantages. These include a higher output voltage level (increasing from 5 levels with two cascaded inverters to 7 levels with three cascaded inverters), a significant decrease in voltage THD (falling from 24.99 % to 15.07 % for the same configurations, respectively) and enhanced torque quality (improving from 0.88 % to 0.45 %). The different degraded mode operating configurations for the OEWIM were investigated with the analysis of the switch failure in one of the two cascaded 2-level inverters. Four configurations are then detailed, along with the operational constraints necessary for each scenario. The resulting simulations confirmed the control strategy's efficacy and underscore the importance of this inverter-machine topology for guaranteeing system service continuity. Furthermore, the system configuration successfully balances the power segmentation capabilities and service continuity achieved by using cascaded two-level inverters with the machine. Moreover, the use of cascaded 2-level inverters to feed the machine makes it possible to withstand a second inverter fault, consequently enhancing the drive system's reliability.

Conflict of interest. The authors declare that they have no conflicts of interest.

REFERENCES

1. Nemouchi B., Rezgui S.E., Benalla H., Nebti K. Fractional-based iterative learning-optimal model predictive control of speed induction motor regulation for electric vehicles application. *Electrical Engineering & Electromechanics*, 2024, no. 5, pp. 14-19. doi: https://doi.org/10.20998/2074-272X.2024.5.02.

2. Chaib Ras A., Bouzerara R., Bouzeria H. An adaptive controller for power quality control in high speed railway with electric locomotives with asynchronous traction motors. *Electrical Engineering & Electromechanics*, 2024, no. 2, pp. 23-30. doi: https://doi.org/10.20998/2074-272X.2024.2.04.

3. Senani F., Rahab A., Benalla H. Performance evaluation and analysis by simulation for sliding mode control with speed regulation of permanent magnet synchronous motor drives in electric vehicles. *Electrical Engineering & Electromechanics*, 2025, no. 5, pp. 43-48. doi: https://doi.org/10.20998/2074-272X.2025.5.06.

4. Guizani S., Nayli A., Ben Ammar F. Comparison between star winding and open-end winding induction machines. *Electrical Engineering*, 2016, vol. 98, no. 3, pp. 219-232. doi: https://doi.org/10.1007/s00202-016-0359-4.

5. Guizani S., Nayli A., Ben Ammar F. Fault-tolerant control of a double star induction machine operating in active redundancy. *Electrical Engineering & Electromechanics*, 2025, no. 6, pp. 27-31. doi: https://doi.org/10.20998/2074-272X.2025.6.04.

6. Nayli A., Guizani S., Ben Ammar F. Experimental analysis for star and open-end stator winding structures of IM. *Power Electronics and Drives*, 2025, vol. 10, no. 1, pp. 271-286. doi: https://doi.org/10.2478/pead-2025-0019.

7. Ebrahimi F., Wndarko N.A., Gunawan A.I. Wild horse optimization algorithm implementation in 7-level packed U-cell multilevel inverter to mitigate total harmonic distortion. *Electrical Engineering & Electromechanics*, 2024, no. 5, pp. 34-40. doi: https://doi.org/10.20998/2074-272X.2024.5.05.

8. Benboukous M., Bahri H., Talea M., Bour M., Abdouni K. Comparative analysis of principal modulation techniques for modular multilevel converter and a modified reduced switching frequency algorithm for nearest level pulse width modulation. *Electrical Engineering & Electromechanics*, 2025, no. 4, pp. 26-34. doi: https://doi.org/10.20998/2074-272X.2025.4.04.

9. Sun J., Zheng Z., Li C., Wang K., Li Y. Optimal Fault-Tolerant Control of Multiphase Drives Under Open-Phase/Open-Switch Faults Based on DC Current Injection. *IEEE Transactions on Power Electronics*, 2022, vol. 37, no. 5, pp. 5928-5936. doi: https://doi.org/10.1109/TPEL.2021.3135280.

10. Abdelwanis M.I., Zaky A.A. Maximum power point tracking in a perovskite solar pumping system with a six-phase induction motor. *Revue Roumaine des Sciences Techniques Serie Electrotechnique et Energetique*, 2024, vol. 69, no. 1, pp. 15-20. doi: https://doi.org/10.59277/RRST-EE.2024.1.3.

11. Chaabane H., Khodja D.E., Chakroune S., Hadji D. Model reference adaptive backstepping control of double star induction machine with extended Kalman sensorless control. *Electrical Engineering & Electromechanics*, 2022, no. 4, pp. 3-11. doi: https://doi.org/10.20998/2074-272X.2022.4.01.

12. L'Hadj Said M., Ali Moussa M., Bessaad T. Control of an autonomous wind energy conversion system based on doubly fed induction generator supplying a non-linear load. *Electrical Engineering & Electromechanics*, 2025, no. 4, pp. 3-10. doi: https://doi.org/10.20998/2074-272X.2025.4.01.

13. Darsouni Z., Rezgui S.E., Benalla H., Rebahi F., Boumendjel M.A.M. Ensuring service continuity in electric vehicles with vector control and linear quadratic regulator for dual star induction motors. *Electrical Engineering & Electromechanics*, 2025, no. 2, pp. 24-30. doi: https://doi.org/10.20998/2074-272X.2025.2.04.

14. Zerdani M., Ardjoun S.A.E.M., Chafouk H., Denai M. Experimental Investigation of Decoupled Discontinuous PWM Strategies in Open-End Winding Induction Motor Supplied by a Common DC-Link. *IEEE Journal of Emerging and Selected Topics in Power Electronics*, 2023, vol. 11, no. 3, pp. 3087-3096. doi: https://doi.org/10.1109/JESTPE.2023.3258799.

15. Yu Z., Chen Y., Zhao J., Zhang X., Zhou X. Alternate Subhexagonal Center Dual-Inverter PWM Scheme for Open-End Winding DC-Biased-VRM Drive Using Adjustable Zero Voltage Vector With Dead-Time Effect Compensation. *IEEE Transactions on Transportation Electrification*, 2025, vol. 11, no. 3, pp. 7322-7333. doi: https://doi.org/10.1109/TTE.2025.3526609.

Received 13.08.2025
Accepted 09.11.2025
Published 02.03.2026

A. Nayli [1,3], *Doctor of Electrical Engineering,*
S. Guizani [2,3], *Professor of Electrical Engineering,*
F. Ben Ammar [3], *Professor of Electrical Engineering,*
[1] University of Gafsa, IPEIG, Tunisia,
e-mail: abdelmonoem.nayli@gmail.com (Corresponding Author)
[2] University of El Manar, IPEIEM, Tunisia.
[3] MMA Laboratory, INSAT, University of Carthage, Tunisia.

How to cite this article:
Nayli A., Guizani S., Ben Ammar F. Normal and degraded operation of the open-end winding induction machine fed by 2-level inverters in cascading. *Electrical Engineering & Electromechanics*, 2026, no. 2, pp. 67-73. doi: https://doi.org/10.20998/2074-272X.2026.2.09